ELSEVIER

Journal of Nuclear Materials 312 (2003) 199–206

journal of nuclear materials

www.elsevier.com/locate/jnucmat

Microstructural modification due to reheating in multipass manual metal arc welds of 9Cr–1Mo steel

R. Mythili, V. Thomas Paul, S. Saroja, M. Vijayalakshmi *, V.S. Raghunathan

Materials Characterisation Group, Physical Metallurgy Section, Indira Gandhi Centre for Atomic Research, Kalpakkam 603102, India

Received 19 December 2001; accepted 19 November 2002

Abstract

The present paper describes the modification of the primary solidification structure of the weld region of a 9Cr–1Mo steel weldment, due to reheating during multipass welding. The 'primary' microstructure is represented by that region of the weld, solidified from the liquid state. In a multipass weld, this microstructure is considerably modified as further layers are deposited on the top and on either side of a pass. The secondary or reheated structure as it is called is sensitive to the welding process parameters and to the physical metallurgical behaviour of the steel. The microstructural evolution depends on the thermal cycle experienced by the weld section due to the two types of deposits, namely one layer over another and passes laid side by side. The observed microstructural variations were correlated to hardness and X-ray FWHM measurements. Thus, the paper presents a study of all the microstructural changes that take place in weld region during multipass welding.

1. Introduction

The use of 9Cr–1Mo steel as steam generator material and a candidate material for core component applications for Fast Breeder Reactors is well established [1,2]. The main reasons have been the adequate mechanical strength at service temperatures [3,4], good corrosion resistance [5,6] and easy control of microstructure through heat treatments [7–9]. The high temperature austenite in this steel transforms to a variety of products depending on the temperature of exposure and the subsequent cooling rate [10,11].

The weldments of this class of steel are susceptible to frequent failures. Very often, failure of a component is initiated in a localised microscopic region of a weldment either during fabrication or during service [12,13]. This could be attributed to differences in the properties of various regions of the weldment, due to the heterogeneity in microstructure, arising due to differences in the thermal cycles undergone by each region during welding [14–17].

In a multipass manual metal arc (MMA) 9Cr–1Mo steel weld the thermal cycles introduced in the solidified structure by the subsequent pass, results in a heterogeneous microstructure, as the weld beads are deposited both side by side as well as one over another. The structure developed is sensitive to variations in the welding process parameters and the physical metallurgical behaviour of the steel. Though the evaluation of microstructure for a given weld is possible, its generalization is valid only under the assumption that the welding parameters like weld bead spacing and overlap between weld beads are maintained reasonably constant. It is normally difficult to control the welding parameters in commercial practice. The observed microstructural variations are therefore unavoidable and can be attributed to the thermal cycles experienced by the weld sections during reheating.

The present paper describes the microstructural variations within the weld region of a 9Cr–1Mo weldment.

* Corresponding author. Tel.: +91-4114 480306; fax: +91-4114 480081.

E-mail address: mvl@igcar.ernet.in (M. Vijayalakshmi).

0022-3115/03/$ - see front matter © 2003 Elsevier Science B.V. All rights reserved.
doi:10.1016/S0022-3115(02)01680-X

The theme of the paper is twofold, to study the microstructural variations

(1) at various planes parallel to the weld centre line at varying distances from it and
(2) at various distances along the weld centre.

A distinct microstructural pattern repeating periodically at various locations in the weld was observed. A detailed investigation on the variation of microstructure, microchemistry and lattice strain along the weld centre line, from top to the bottom, is presented in this paper. The recovery of strain due to tempering effects in various regions of the weld has also been studied. Thus, the paper presents a comprehensive description on the microstructural changes in the weld region of a 9Cr–1Mo weldment during reheating due to multiple passes.

2. Experimental details

The 9Cr–1Mo steel MMA weldments were fabricated from normalized and tempered plates procured from Creusot Loire, France. The composition of the steel and welding conditions are listed in Tables 1 and 2 respectively. Fig. 1(a) gives the geometry of the weldment, while Fig. 1(b) shows the region chosen to study of effect of multipass. The classification as top, middle and root, shown in the schematic (Fig. 1(b)) has been adopted in this study to represent regions in the weld at distances of about 0–3, 4–7 and 8–12 mm respectively from the top surface of the 9Cr–1Mo plate. The term root in the present study refers to locations at the bottom of the weld region and does not pertain to any specific pass for the limited purpose of studying the effect of high temperature exposure or tempering along the weld centre line.

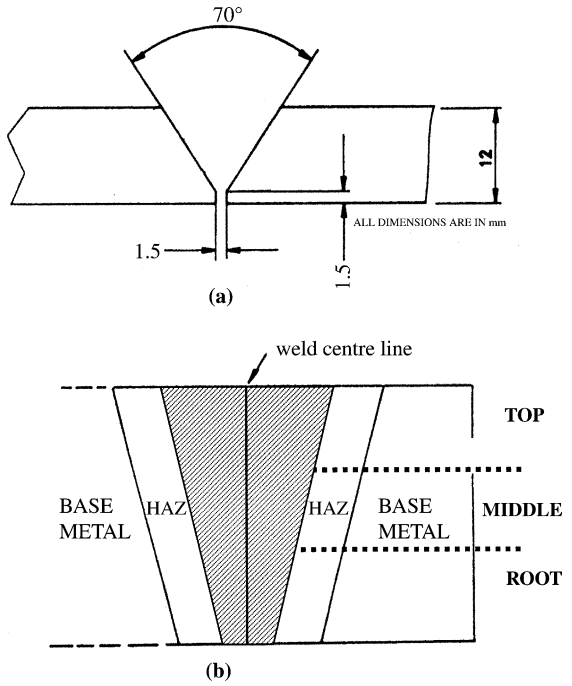

Fig. 1. (a) Geometry of the weld, (b) region of weld chosen to study effect of multipass. A classification of top, middle and root has been used for the study of tempering effects along the weld centre line.

Table 1
Composition of steel used

Element	Composition in wt%
Chromium	8.24
Molybdenum	0.955
Manganese	0.356
Carbon	0.072
Phosphorus	0.021
Silicon	0.265
Sulphur	0.008
Iron	Balance

Table 2
Welding parameters

Parameter	Description
Welding process	Manual metal arc
Electrode	Basic coated 9Cr–1Mo electrodes
Composition of the electrode (in wt%)	Cr = 8.9, Mo = 0.98, C = 0.12, Si = 0.52, Mn = 0.52, P = 0.003, S = 0.03, Fe = balance
Arc voltage	22 V
Arc current	100–130 A
No. of passes	Four

The samples for optical and scanning electron microscopy (SEM) were prepared by standard metallographic methods. The SEM analysis was carried out using a Philips SEM model-PSEM 501 on gold-coated samples and the grain size was measured by the linear intercept method. Analytical transmission electron microscopy (ATEM) analyses, using a Philips CM 200 TEM with EDAX (super ultra thin window) and DX4 analyzer, was carried out for identification of carbides and determination of microchemistry using carbon extraction replicas; details of the analysis are discussed elsewhere [18,19]. The variation of lath size, from top to root along the weld centre line was estimated by TEM using thin foils, and is listed in Table 3, along with the

Table 3
Variation of lath size along weld centre line

S. no.	Region	Lath size/μm $\Sigma \pm 10\%$
1	Top (2 mm from top)	0.11
2	Middle (5 mm from top)	0.24
3	Root (8 mm from top)	0.36

Table 4
Microchemistry and number density of carbides along weld centre line

S. no.	Region	Type of carbide	Elements in metal sublattice (at.%) $\Sigma = \pm 10\%$			No. density of carbides/μm^2
			Fe	Cr	Mo	
1	Top	$M_{23}C_6$	53	20	27	Very few
2	Middle	$M_{23}C_6$	21	47	32	1–2
3	Root	$M_{23}C_6$	36	57	7	5–6

error limits. The AEM data on percentage of elements (average of Cr, Fe and Mo contents) measured from several carbides is given in Table 4. The microhardness measurements and evaluation of lattice strain from X-ray FWHM measurements were carried out using a Leitz Miniload II Microhardness Tester and Philips diffractometer, respectively.

3. Results and discussion

The microstructure developed in the weld as the liquid pool cools to ambient temperature is referred to as the 'primary solidification' or the 'as welded' structure. Therefore, in a multipass weld, only the top surface of the weld represents the primary solidification structure. This structure was established by extensive analytical electron microscopy studies on 10 different cross-sections of the weldment (parallel to weld centre line) and the distinct microstructural zones are illustrated as a schematic microstructural map [19] in Fig. 2. It can be seen that the weld region consists of martensite (α'), the HAZ consists of a range of microstructures, while the base metal refers to the unaffected portion of the weldment. The changes in the concentration of chromium and molybdenum in ferrite across the various cross-sections, estimated by ATEM analysis, are presented elsewhere [19]. The description of the primary structure alone is inadequate to understand the true structure of the multipass MMA weld. In reality, the reheating of the primary structure to high temperatures as the weld beads are deposited side by side and one above the other would initiate reversion of martensite (α') either completely or at least partially to austenite, resulting in a structure, different from the primary structure, when cooled subsequently. This structure of the weld called the 'reheated' or 'secondary solidification' structure will be described in detail here.

3.1. Secondary solidification structure

The microstructural changes in the weld region depends on the thermal cycles experienced by the weld due to the deposits laid side by side and one above the other. Therefore, detailed microscopic investigation was carried out on a section of the weld as shown in Fig. 1(b).

A careful observation on the above surface at different distances suggested a distinct pattern of microstructure repeating periodically. Fig. 3(a)–(d) shows a typical sequence of such microstructures. The columnar

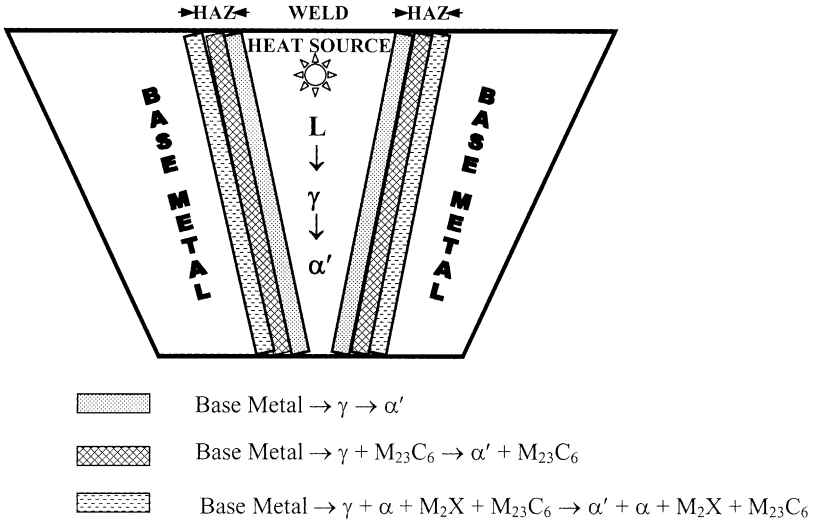

Fig. 2. Schematic of microstructural zones in primary solidification structure of weldment.

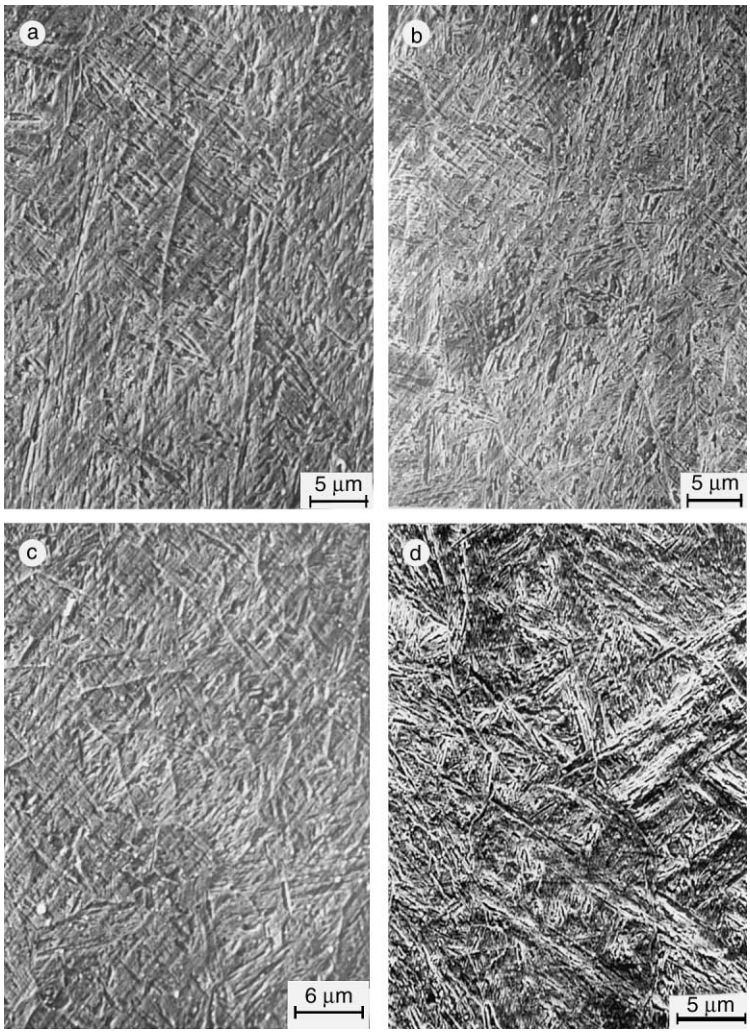

Fig. 3. Effect of multipass on primary solidification structure. Repetitive microstructure observed within the weld region: (a) columnar, (b) coarse grains of γ, (c) fine grains of γ and (d) the unaffected region.

grains (length: 180 ± 10 μm; width: 44 ± 4 μm) in Fig. 3(a) represents regions that have witnessed temperatures above the liquidus and have cooled rapidly. Fig. 3(b) shows coarse γ grains (size: 72 ± 5 μm) corresponding to regions reaustenitised at high temperature in the single austenite phase field that has led to unrestricted growth of γ grains. The third region shown in Fig. 3(c) is fine grained (size: 18 ± 2 μm), since the range of temperatures witnessed by this region is not very high, probably close to Ac_3 or between Ac_3 and Ac_1. The regions shown in Fig. 3(d) have not undergone any observable microstructural modification, implying that they could be at larger distances from the heat source. The microstructures corresponding to four regions clearly reveal structures with columnar grains, coarse grains, fine grains and unaffected structure respectively. This observation suggests modification of the primary structure depending on the temperatures witnessed, welding speed and distance from the heat source as each further pass or layer is made. However, each pass influences only a very small region (Fig. 4) of the previous pass, below which remains the unaffected structure.

The hardness variation measured perpendicular to the weld centre line along the middle portion of the weldment also reflects this behaviour (Fig. 5). The hardness values within the weld region show a periodic variation, though a direct correlation with the microstructural variations could not be made, as the hardness measurements were taken at intervals of 100–200 μm, which is higher than the width of these zones. However, the trend confirms that there is a repetitive pattern in the microstructure. This observation of a repetitive micro-

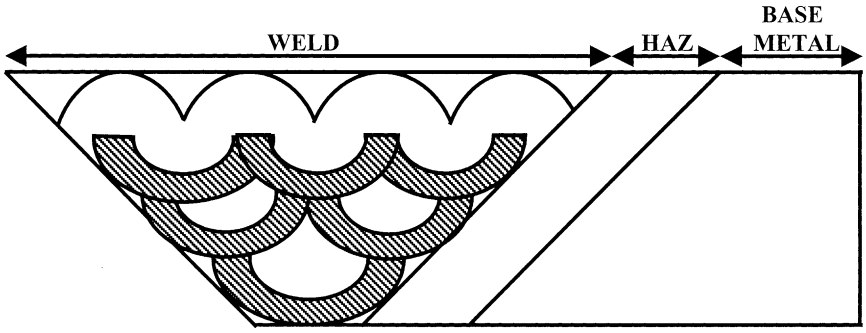

Fig. 4. Schematic representation of multipass profiles. The shaded region in each of the multipass profile represents the region over which the structure is modified due to reheating.

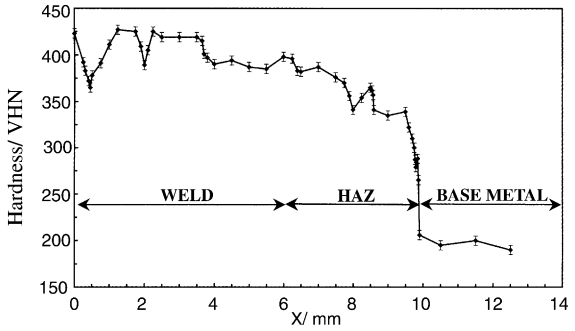

Fig. 5. Hardness variation as a function of distance from the weld centre line.

structure at regular distances suggest that the condition for complete reaustenitisation as proposed by the Reed and Bhadeshia [20] model, is satisfied in the present study.

3.2. Microstructural variation along weld centre line

The effect of reheating on the primary structure manifests itself in a number of ways, like decrease in the defect density, coarsening of laths, grain growth and precipitation of carbides. Reheating of the weld was studied in three regions along the weld centre line, namely top (about 2 mm from the top), middle (about 5 mm from the top) and root (about 8 mm from the top) as shown in Fig. 1(b). The results of these studies are described below.

3.2.1. Heterogeneity of microstructure and microchemistry along weld centre line

Transmission electron micrographs on thin foils, from the above three regions are shown in Fig. 6(a)–(c). A martensite with fine laths (Fig. 6(a)) at the top, coarser laths in the middle region (Fig. 6(b)) and formation of cells and subgrains in the root region (Fig. 6(c)) are observed, suggesting the onset of recovery towards the root portion. An increase in the lath width

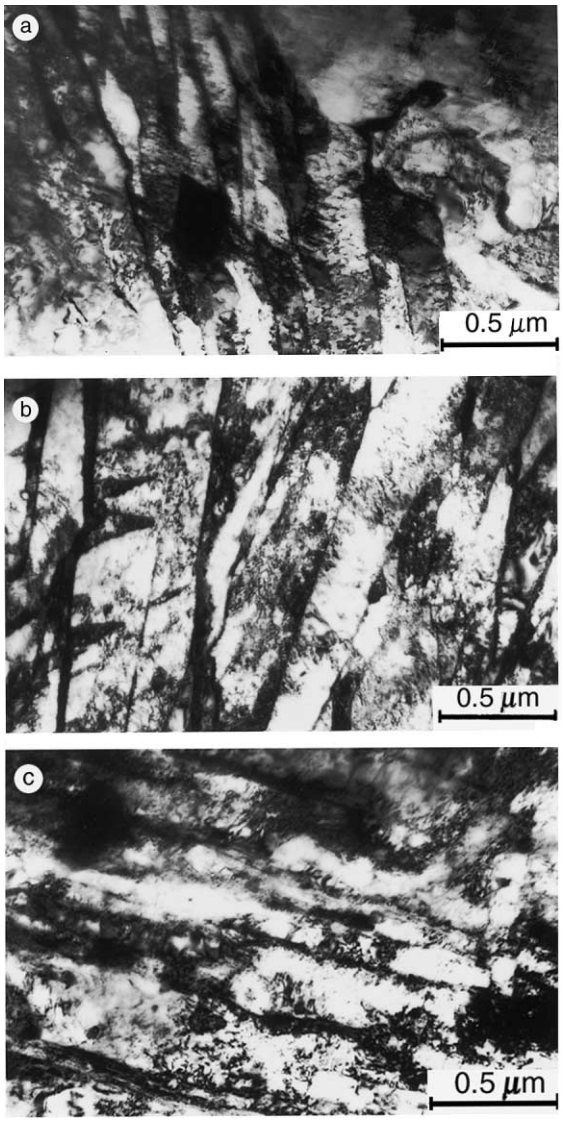

Fig. 6. TEM micrographs of thin foils from top to root of the weld showing coarsening of laths: (a) top, (b) middle and (c) root.

from 0.11 μm at the top to about 0.36 μm near the root (Table 3) is observed, which confirms that the root region has undergone tempering due to high temperature exposure.

The tempering of martensite during reheating leads to the precipitation of carbides. ATEM analysis (Fig. 7(a)–(f)) on carbon extraction replicas from regions along the weld centre line show the presence of few, very fine carbides in the top region (Fig. 7(a)), with a gradual increase in the size and number density of carbides, as the root portion or bottom of the weld is approached (Fig. 7(c) and (e)). The number density and microchemical details of the carbides are given in Table 4. Due to the small size of carbides in the top region, their identification by microdiffraction or selected area diffraction could not be carried out. However, detailed analysis of a very large number of carbides in 9Cr–1Mo steel have shown [7,10,21,22] that $M_{23}C_6$ and M_2X are the only two types of carbides that form in this steel, where M includes the metal atoms Cr, Fe and Mo. $M_{23}C_6$ though generally chromium rich can accommodate varying amounts of iron, depending on its temperature and time of formation. The microchemistry, especially the chromium content in M of $M_{23}C_6$ has been established as a fingerprint for identification of the temperature and time of formation of carbide [18,19,23]. It has been established in our earlier studies that the chromium content in M of M_2X was always around 90% in contrast to around a maximum of 60% in a Cr rich $M_{23}C_6$ carbide [7,22,24]. This difference in chromium content between M_2X and $M_{23}C_6$ is used as an index to distinguish between the two types of carbides.

It was seen in our earlier studies [25] on wrought 9Cr–1Mo steel, that tempering the martensite at 823 K

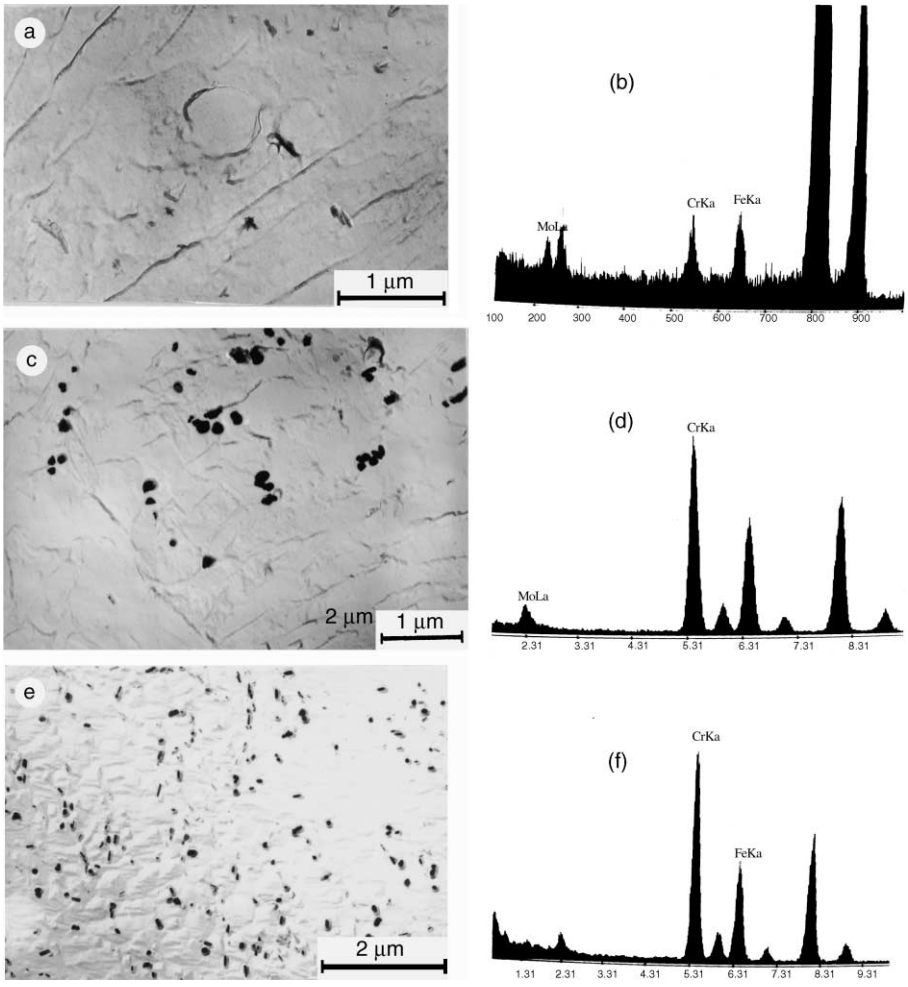

Fig. 7. Microstructural inhomogeneity along weld centre line from top to root. TEM micrograph of carbon extraction replica and EDS spectrum from a carbide in the region. (a,b) Top, (c,d) middle and (e,f) root portion. An increase in the Cr/Fe content in the $M_{23}C_6$ carbide is seen from the top to the root.

led to the formation of only $M_{23}C_6$, with the Cr/Fe content increasing with time. M_2X did not form at 823 K, while it formed after about 75 h of aging at 923 K, though $M_{23}C_6$ formed very rapidly. The formation of M_2X within an hour of tempering at 1023 K along with $M_{23}C_6$ was observed. Therefore, the carbides in the top region of the weld could be classified as $M_{23}C_6$ type, but rich in iron (Fig. 7(b)), though diffraction evidence could not be obtained. The Fe rich nature of the $M_{23}C_6$ carbide is attributed to its mechanism of formation i.e. forming under non-equilibrium conditions in the lower temperature range ~823 K [23]. This is due to a fast cooling rate and insufficient time for chromium to diffuse into the precipitates. Under these cooling conditions, M_2X is not expected to form.

The carbides in the middle and root region are also identified as $M_{23}C_6$ carbides from the analysis of energy dispersive spectrometry (EDS) spectra taken from a large number of precipitates (Fig. 7(d) and (f)). These carbides are rich in chromium implying that chromium diffusion has taken place. The higher chromium content in $M_{23}C_6$ from the root region suggests that these regions have experienced temperatures close to tempering temperatures, enabling diffusion of chromium into the precipitates [7,18], than the regions above.

3.2.2. Variation of lattice strain along weld centre line

The observed microstructural and microchemical variations was a manifestation of the extent of tempering along the weld centre line. An attempt was made to evaluate the lattice strain using the full width at half maximum (FWHM) from the X-ray diffraction peaks of α-Fe, as a parameter sensitive to the variation in lattice strain. A strain parameter '*S*' is calculated using the following equation:

$$S = \left(\frac{\Delta\text{FWHM}}{\text{FWHM}_{\text{bm}}}\right) \times 100, \quad (1)$$

where ΔFWHM refers to the difference in the value of FWHM from the region of interest, say top, middle or root and reference, $(\text{FWHM})_{\text{bm}}$ refers to that of the base metal, which is taken as the reference. Table 5 shows the value of '*S*' and the variation in hardness from top to root. The hardness variation – a combined manifestation of factors like defect density, substructure, precipitation, etc. shows, a gradual decrease from top to root, suggesting that the extent of tempering is higher as the root is approached. The decrease in FWHM, from top to root is consistent with the decrease in hardness. These observations suggest that there is considerable tempering of the structure due to reheating during multipass welding.

Table 5
Variation of lattice strain and microhardness along the weld centre line

S. no.	Region	S (%)	Microhardness VHN (load = 100 g)
1	Top	33	438
2	Middle	33	444
3	Root	25	384

4. Conclusion

This paper describes the two themes of the secondary solidification structure in a MMA welded 9Cr–1Mo steel. The main conclusions are as follows:

- The presence of a 'repetitive microstructure' consisting of columnar grain, coarse grained austenite, fine grained austenite and unaffected structure within the weld zone confirms that there is a significant modification of microstructure due to multiple passes.
- Studies along the weld centre line from top to root suggest that there is significant coarsening of laths, decrease in defect density and extensive precipitation with Cr enrichment in the carbides. The variation in lattice strain evaluated using X-ray FWHM values correlate well with the observed microstructural variations. These studies suggest extensive tempering of the primary solidification structure as the root is approached.

Acknowledgements

The authors wish to acknowledge the keen and constant encouragement shown by Dr Baldev Raj, Director, Materials, Chemistry and Reprocessing Group and Dr Placid Rodriguez, Former Director, IGCAR, Kalpakkam in the pursuit of their studies on ferritic steels.

References

[1] E.A. Little, Proceedings of the International Conference on Materials for Nuclear Core Applications, vol. 2, BNES, London, 1987, p. 47.
[2] J. Orr, F.R. Beckitt, G.D. Fawkes, in: S.F. Pugh, E.A. Little (Eds.), Proceedings of the International Conference on Ferritic Steels for Fast Reactor Steam Generators, BNES, London, 1978, p. 91.
[3] C. Willby, J. Walters, in: S.F. Pugh, E.A. Little (Eds.), Proceedings of the International Conference on Ferritic Steels for Fast Reactor Steam Generators, BNES, London, 1978, p. 40.

[4] M.K. Booker, V.K. Sikka, B.L.P. Booker, in: Ashok Khare (Ed.), Proceedings of the International Conference on Production, Fabrication, Properties and Application of Ferritic Steels for High Temperature Applications, ASM, Metals Park, OH, 1982, p. 257.
[5] J.A.G. Holmes, Nucl. Energy 20 (1) (1981) 23.
[6] H. Nickel, P.J. Ennis, W.J. Quadakkers, Trans. IIM 50 (6) (1997) 681.
[7] S. Saroja, M. Vijayalakshmi, V.S. Raghunathan, Mater. Trans. JIM 34 (1993) 901.
[8] P. Parameswaran, M. Vijayalakshmi, P. Shankar, V.S. Raghunathan, J. Mater. Sci. 27 (1992) 5426.
[9] S. Saroja, M. Vijayalakshmi, V.S. Raghunathan, Mater. Sci. Eng. A 154 (1992) 59.
[10] S. Saroja, M. Vijayalakshmi, V.S. Raghunathan, J. Mater. Sci. 27 (1992) 2389.
[11] F.B. Pickering, A.D. Vassiliou, Met. Technol. 7 (1980) 409.
[12] T. Oldland, C.W. Ramsay, D.K. Matlock, D.L. Olson, Weld. Res. Suppl. (April) (1989) 158s.
[13] M. Dewitte, C. Coussement, Mater. High Temp. 9 (4) (1991) 178.
[14] J.G. Zhang, F.W. Noble, B.L. Eyre, Mater. Sci. Technol. 7 (1991) 315.
[15] K. Laha, K.B.S. Rao, S.L. Mannan, Mater. Sci. Eng. A 129 (1990) 183.
[16] R.S. Fidler, D.J. Gooch, in: S.F. Pugh, E.A. Little (Eds.), Proceedings of the International Conference on Ferritic Steels for Fast Reactor Steam Generators, BNES, London, 1978, p. 128.
[17] P. Roy, T. Lauritzen, Weld. Res. Suppl. (February) (1986) 45s.
[18] M. Vijayalakshmi, PhD thesis, University of Madras, 1997.
[19] M. Vijayalakshmi, S. Saroja, V. Thomas Paul, R. Mythili, V.S. Raghunathan, Metall. Mater. Trans. 30A (1999) 161.
[20] R.C. Reed, H.K.D.H. Bhadeshia, Acta Metall. Mater. 42 (11) (1994) 3663.
[21] B.A. Senior, F.W. Noble, B.L. Eyre, Acta Metall. Mater. 36 (1988) 1855.
[22] S. Saroja, P. Parameswaran, M. Vijayalakshmi, V.S. Raghunathan, Acta Metall. Mater. 43 (8) (1995) 2985.
[23] M. Vijayalakshmi, S. Saroja, V. Thomas Paul, R. Mythili, V.S. Raghunathan, J. Nucl. Mater. 279 (2000) 293.
[24] S. Saroja, M. Vijayalakshmi, V.S. Raghunathan, Trans. IIM 48 (3) (1995) 271.
[25] S. Saroja, PhD thesis, University of Madras, 1999.